Intelligent Automation And Soft Computing, 2020
Vol.26,no.3, 439–446
DOI: 10.32604/iasc.2020.013920

Intelligence-based Channel Equalization for 4x1 SFBC-OFDM Receiver

Divneet Singh Kapoor[1,*], Amit Kumar Kohli[2]

[1] Electronics and Communication Engineering Department, Chandigarh University, Mohali-140413, Punjab, India.
[2] Electronics and Communication Engineering Department, Thapar Institute of Engineering and Technology, Patiala-147001, India.

ABSTRACT

This research paper represents an intelligent receiver based on the artificial-neural-networks (ANNs) for a 4x1 space-frequency-block-coded orthogonal-frequency-division-multiplexing (SFBC-OFDM) system, working under slow time-varying frequency-selective fading channels. The proposed equalizer directly recovers transmitted symbols from the received signal, without the explicit requirement of the channel estimation. The ANN based equalizer is modelled by using feedforward as well as the recurrent neural-network (NN) architectures, and is trained using error backpropagation algorithms. The major focus is on efficiency and efficacy of three different strategies, namely the gradient-descent with momentum (GDM), resilient-propagation (RProp), and Levenberg-Marquardt (LM) algorithms. The recurrent neural network architecture based SFBC-OFDM system is found to be an appropriate choice in terms of the low bit-error-rate performance, while using different quasi-orthogonal space-time block codes.

KEY WORDS: ANN, backpropagation, SFBC-OFDM.

1 INTRODUCTION

THE performance of the MIMO-OFDM systems has improved with the usage of coding schemes, such as SFBC (Lee & Williams, 2000). For more than two-transmitters, the coding schemes exhibit either low code-rate or the quasi-orthogonal (QO) with reduced diversity-gain. Prior to detection of the data symbols, the conventional channel estimation techniques utilized in the communication systems are the least-squares (LS) and the minimum-mean-square-error (MMSE). The heuristic approaches for channel estimation and equalization, which employ ANNs, have also been utilized due to their universal approximation and learning ability (Haykin, 2009). As a nonlinear classifier, ANNs can be used to form nonlinear decision boundaries, and these can estimate a nonlinear wireless fading channel for compensation. For the MIMO-OFDM systems, the neural-network with feedback is reported for reliable channel estimation by Seyman & Taspinar (2012), which utilizes the backpropagation (BP) algorithm for network training. For the space-time coded OFDM systems, the channel estimation can be performed using a feedforward multilayered perceptron network (Seyman & Taspinar, 2013). But, it is also advantageous to incorporate the ANNs directly for channel equalization, without the explicit requirement of the channel estimation (Ye, Li, & Juang, 2018), in which, deep neural networks are utilized for signal detection, because of their ability to learn the characteristics of channels without online training.

ANNs can be structured as a feedforward (without feedback), or recurrent (with feedback loop) (Haykin, 2009). The presence of the feedback loop in recurrent architectures tends to boost the learning capability of the network. The most common learning algorithm is the gradient-descent-with-momentum (GDM), in which, the weight-update is stabilized and accelerated using the influence of the previous step on the current update (by minimizing the error between the network outputs and the desired response) (Haykin, 2009). As the weight-update is also dependent on the partial derivative of the error function w.r.t. weight vector, the resilient-propagation (RProp) algorithm makes the weight-update size vary according to the behavior of the partial derivative (Riedmiller & Braun, 1993). Another category of learning algorithms utilizes the standard optimization techniques to minimize the error energy as a function of weights, like the Levenberg-Marquardt (LM) algorithm, which is a modification of Gauss-Newton method for the application of a nonlinear LS algorithm (Hagan & Menhaj, 1994).

This research paper addresses an ANN based receiver for the 4×1 SFBC-OFDM system using the backpropagation algorithm for the network training,

CONTACT Divneet Singh Kapoor divneet.singh.kapoor@gmail.com

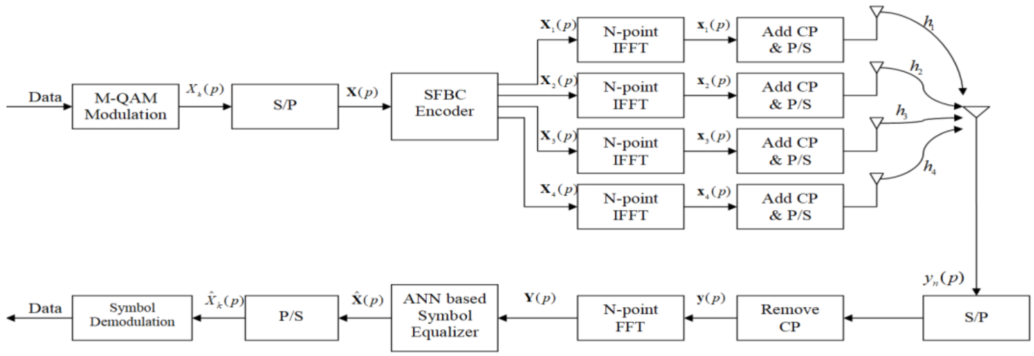

Figure 1. Model for the Underlying 4x1 SFBC-OFDM System.

which directly recovers the transmitted symbols from the received signal. The conventional matched-filtering (MF) equalization approach, even with a perfectly known channel, introduces interference from the adjacent symbols, because of QO-codes. The feedforward (FFNN) as well as the recurrent (RNN) network architectures are explored as intelligent receivers for the underlying system, while utilizing various learning algorithms for the intended equalization. The bit-error-rate (BER) performance evaluation of the underlying SFBC-OFDM system is also analyzed (through Monte-Carlo simulation) using distinct QO-STBC schemes (Hou, Lee, & Park, 2003).

2 SFBC-OFDM SYSTEM MODEL

IN an SFBC-OFDM system (as shown in Figure 1), the serial stream of the binary data is taken as an input to the underlying system, and it is first mapped to the M-ary quadrature-amplitude-modulation (M-QAM) to generate information symbols. These symbols are collected in a serial-to-parallel converter to form a symbol vector as: $\mathbf{X}(p)=\left[X_0(p),X_1(p),...,X_{N-1}(p)\right]^T_{N\times1}$, where $[.]^T$ is matrix transposition operator and p is block index. The symbol vector is then fed to an SFBC encoder, which generates the coded sequence vectors (of length N) for each of the M_T number of transmitters, to utilize the space-frequency diversity. The QO-coded sequence vectors, for $M_T=4$ transmitters (Jafarkhani, 2001), are given as:

$$\begin{aligned}
\mathbf{X}_1(p)&=\left[..,X_{4m}(p),-X^*_{4m+1}(p),-X^*_{4m+2}(p),X_{4m+3}(p),..\right]^T_{N\times1}\\
\mathbf{X}_2(p)&=\left[..,X_{4m+1}(p),X^*_{4m}(p),-X^*_{4m+3}(p),-X_{4m+2}(p),..\right]^T_{N\times1}\\
\mathbf{X}_3(p)&=\left[..,X_{4m+2}(p),-X^*_{4m+3}(p),X^*_{4m}(p),-X_{4m+1}(p),..\right]^T_{N\times1}\\
\mathbf{X}_4(p)&=\left[..,+X_{4m+3}(p),X^*_{4m+2}(p),+X^*_{4m+1}(p),X_{4m}(p),..\right]^T_{N\times1}
\end{aligned} \tag{1}$$

For $m=0,1,...,(N/4)-1$, where, $(.)^*$ denotes the complex conjugation operator. The coded sequence vectors $\mathbf{X}_i(p)=\left\{X_{i,k}(p)\right\}_{k=0}^{N-1}$ are then mapped on to the N-subcarriers via the inverse-fast-Fourier-transform (IFFT) to form transmit sequences, $\mathbf{x}_i(p)=\left[x_{i,0}(p),x_{i,1}(p),...,x_{i,N-1}(p)\right]^T_{N\times1}$; where $x_{i,n}(p)=\left(1/\sqrt{N}\right)\sum_{k=0}^{N-1}X_{i,k}(p)\exp\left(j2\pi kn/N\right)$, for $i=1,2,3,4$, with $X_{i,k}(p)$ as the k^{th} symbol of p^{th} block of i^{th} transmit sequence, as in (1). Each $\mathbf{x}_i(p)$ is processed to have a cyclic-prefix (CP) of length G, which is larger than the delay spread of channel L (number of multi-paths) (Kohli & Kapoor, 2016). The transmitted SFBC-OFDM signal encounters the time-varying fading channel, which is assumed to remain static for one CP-OFDM block period. Its tap-coefficients are considered to follow the second-order autoregressive (AR2) process (Kohli & Mehra, 2006; Singh & Kohli, 2014), as:

$$h_{i,l}(p)=-K_1h_{i,l}(p-1)-K_2h_{i,l}(p-2)+v_{i,l}(p) \tag{2}$$

Where, $h_{i,l}(p)$ is the channel tap-coefficient for the l^{th} path (with $L=4$) while the transmission of the p^{th} block through i^{th} transmitter $v_{i,l}(p)$ is the complex zero-mean white Gaussian noise. The scalar coefficients are considered to be $K_1=-2r_D\cos\left(\sqrt{2}\pi f_DT_1\right)$ and $K_2=r_D^2$ with $r_D=1-2f_DT_1$, f_D is the maximum Doppler shift, f_DT_1 is the fade-rate, $T_1=(N+G)T_s$ is the CP-OFDM symbol block period, and T_s is the M-QAM information symbol duration (i.e., equivalent to the sampling period). After removal of the CP, the received signal $y_n(p)$ is processed using an N-point FFT operator to obtain the symbols as:

$$Y_k(p)=\sum_{i=1}^{4}H_{i,k}(p)X_{i,k}(p)+W_k(p) \tag{3}$$

where, $H_{i,k}(p)$ for $k=0,1,...,N-1$ corresponds to the FFT of the channel impulse response between the i^{th} transmitter antenna and receiver; $W_k(p)$ is the zero-mean additive-white-Gaussian-noise with variance σ_w^2. When channel gains between adjacent subcarriers are approximately equal i.e.,

$$\begin{bmatrix} Y_{4m}(p) \\ Y^*_{4m+1}(p) \\ Y^*_{4m+2}(p) \\ Y_{4m+3}(p) \end{bmatrix} = \begin{bmatrix} W_{4m}(p) \\ W^*_{4m+1}(p) \\ W^*_{4m+2}(p) \\ W_{4m+3}(p) \end{bmatrix} + \begin{bmatrix} H_{1,4m}(p) & H_{2,4m}(p) & H_{3,4m}(p) & H_{4,4m}(p) \\ H^*_{2,4m}(p) & -H^*_{1,4m}(p) & H^*_{4,4m}(p) & -H^*_{3,4m}(p) \\ H^*_{3,4m}(p) & H^*_{4,4m}(p) & -H^*_{1,4m}(p) & -H^*_{2,4m}(p) \\ H_{4,4m}(p) & -H_{3,4m}(p) & -H_{2,4m}(p) & H_{1,4m}(p) \end{bmatrix} \begin{bmatrix} X_{4m}(p) \\ X_{4m+1}(p) \\ X_{4m+2}(p) \\ X_{4m+3}(p) \end{bmatrix} \quad (4)$$

$H_{i,4m}(p) \approx H_{i,4m+1}(p) \approx H_{i,4m+2}(p) \approx H_{i,4m+3}(p)$ for $i = 1,2,3,4$ (Rouquette, Mérigeault, & Gosse, 2002), the equation (3) can be expressed as equation (4) or equivalently above the equation in a vector/matrix form then:

$$\tilde{\mathbf{Y}}_{4m}(p) = \tilde{\mathbf{H}}_{4m}(p)\tilde{\mathbf{X}}_{4m}(p) + \tilde{\mathbf{W}}_{4m}(p) \quad (5)$$

The QO-codes retain full code-rate with reduced diversity gain. The conventional application of the MF for the symbol decoding leads to

$$\begin{aligned} \hat{\mathbf{X}}_{4m}(p) &= \tilde{\mathbf{H}}^H_{4m}(p)\tilde{\mathbf{Y}}_{4m}(p) \\ &= \tilde{\mathbf{H}}^H_{4m}(p)\tilde{\mathbf{H}}_{4m}(p)\tilde{\mathbf{X}}_{4m}(p) + \tilde{\mathbf{H}}^H_{4m}(p)\tilde{\mathbf{W}}_{4m}(p) \\ &= \begin{bmatrix} \gamma & 0 & 0 & \beta \\ 0 & \gamma & -\beta & 0 \\ 0 & -\beta & \gamma & 0 \\ \beta & 0 & 0 & \gamma \end{bmatrix} \tilde{\mathbf{X}}_{4m}(p) + \tilde{\mathbf{H}}^H_{4m}(p)\tilde{\mathbf{W}}_{4m}(p) \end{aligned} \quad (6)$$

where $(.)^H$ is the Hermitian transpose operator, and the parameter $\gamma = |H_{1,4m}(p)|^2 + |H_{2,4m}(p)|^2 + |H_{3,4m}(p)|^2 + |H_{4,4m}(p)|^2$ depicts diversity gain, and the interference term is indicated by the parameter of $\beta = 2\,\mathrm{Re}\left\{H^*_{1,4m}(p)H_{4,4m}(p) - H^*_{2,4m}(p)H_{3,4m}(p)\right\}$. The need for appropriate symbol decoding motivates the usage of the ANN for intended channel equalization in the underlying SFBC-OFDM system.

3 ANN BASED EQUALIZATION

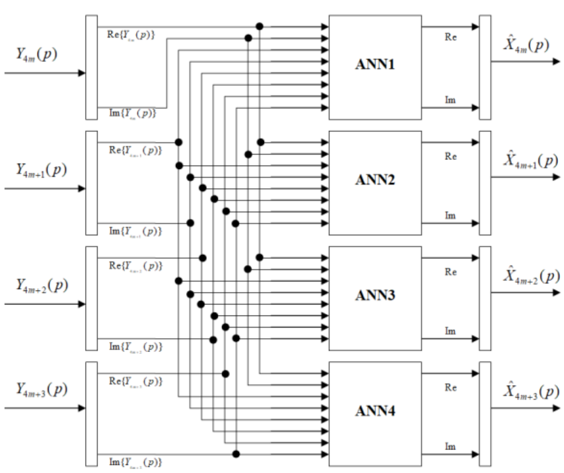

Figure 2. ANN based Model for Equalization in the 4x1 SFBC-OFDM System (Nawaz, Mohsin, & Ikram, 2009).

The ANNs learn about the fading environment by adjusting synaptic weights with the help of training the algorithms, in order to provide a desired response for a given stimuli. The network paradigm employed for equalization in the 4×1 SFBC-OFDM system is illustrated in Figure 2, in which, there are 4 independent NNs for recovering the symbols transmitted from each transmitter. During training, the complex-valued received symbol $\tilde{\mathbf{Y}}_{4m}(p)$ are split into real and imaginary parts, and then fed to the input layer of each ANN block, since a neural network efficiently processes only real symbols. Thus, each network has 8 input and 2 output-nodes (real and imaginary), which are combined to form a complex-valued estimate of the transmitted symbol (Nawaz, Mohsin, & Ikram, 2009). The training sample, utilized to train the ANN in a supervised manner, is denoted as: $\left\{\tilde{\mathbf{Y}}_{4m}(p), X_{4m}(p)\right\}_{p=1}^{P}$. Considering $\hat{X}_{4m}(p)$ as the symbol produced at output of the ANN, the error signal generated at each output node is:

$$\begin{aligned} e_1(p) &= \mathrm{Re}\{X_{4m}(p)\} - \mathrm{Re}\{\hat{X}_{4m}(p)\} \\ e_2(p) &= \mathrm{Im}\{X_{4m}(p)\} - \mathrm{Im}\{\hat{X}_{4m}(p)\} \end{aligned} \quad (7)$$

where, $\mathrm{Re}\{x\}$ and $\mathrm{Im}\{x\}$ indicate the real and imaginary parts of the complex-valued x respectively. Total instantaneous error energy of the network is represented as:

$$\xi(p) = 0.5\left[e_1^2(p) + e_2^2(p)\right] \quad (8)$$

For batch learning, the synaptic weights of the network are adjusted based on the average error energy over the training sample as:

$$\xi_{av} = (1/P)\sum_{p=1}^{P}\xi(p) = (0.5/P)\sum_{p=1}^{P}\left[e_1^2(p) + e_2^2(p)\right] \quad (9)$$

where P is the number of SFBC-OFDM symbol blocks utilized as the training sample (epoch).

3.1 Network Architectures

THE FFNN (Haykin, 2009) consists of an input layer of 8 nodes, two hidden layers of 16 and 8 nodes respectively, and an output layer of 2 nodes. For the RNN (shown in Figure 3), the number of input and output nodes are same as in the FFNN. There is only one hidden layer (of 8 neurons) with a feedback loop. For both hidden layers, the squashing function is sigmoid with values in the range –1 to +1 (hyperbolic tangent function) i.e. $f_{Sig}(r) = \tanh(r)$; and for the output layer, it is the linear function i.e. $f_{Lin}(r) = r$.

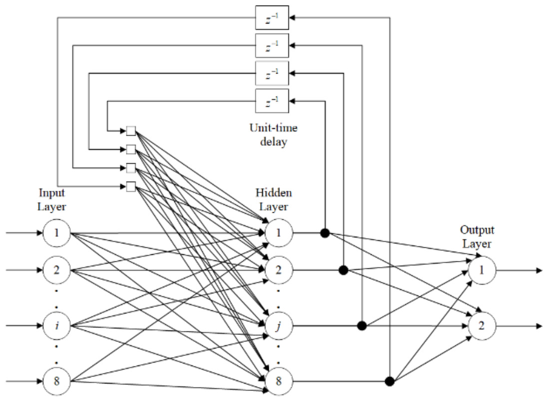

Figure 3. RNN Architecture (Haykin, 2009).

3.2 Training Algorithms

ANN models are trained by assuming the SFBC OFDM modulation and fading channels as black boxes. The BP algorithm (Haykin, 2009) adjusts the weight of connection from i^{th} neuron to j^{th} neuron in the q^{th} layer of the NN, denoted as $\theta_{ji}^{(q)}$, by applying a correction $\Delta\theta_{ji}^{(q)}$, which is proportional to the partial derivative $\partial\xi_{av} / \partial\theta_{ji}^{(q)}$ (9). The synaptic weights are updated as:

$$\theta_{ji}^{(q)}(n_{ep}+1) = \theta_{ji}^{(q)}(n_{ep}) + \Delta\theta_{ji}^{(q)}(n_{ep}) \tag{10}$$

where, n_{ep} is the epoch/iteration index. The performance of the GDM (Haykin, 2009), RProp (Riedmiller & Braun, 1993) and LM (Hagan & Menhaj, 1994) algorithms is compared in terms of the bit-error-rate (BER) of the SFBC-OFDM system. For the appropriate convergence of the BP algorithm, the synaptic weight-adjustment/update for the GDM algorithm (Haykin, 2009) is given as:

$$\Delta\theta_{ji}^{(q)}(n_{ep}) = \alpha\Delta\theta_{ji}^{(q)}(n_{ep}-1) + \eta\left(\partial\xi_{av} / \partial\theta_{ji}^{(q)}(n_{ep})\right) \tag{11}$$

where, α is a momentum constant, and η is learning-rate, which controls the convergence-rate of the algorithm. In order to avoid any problem of the update disturbance due to unforeseeable behaviour of the derivative term in (11), the RProp algorithm changes the weight update size, (which will be subtracted/added to the weight based on the sign of partial derivative) (Riedmiller & Braun, 1993) as:

$$\Delta\theta_{ji}^{(q)}(n_{ep}) = \begin{cases} \eta^{+}\Delta\theta_{ji}^{(q)}(n_{ep}-1) & , \dfrac{\partial\xi_{av}}{\partial\theta_{ji}^{(q)}}(n_{ep}-1)\dfrac{\partial\xi_{av}}{\partial\theta_{ji}^{(q)}}(n_{ep}) > 0 \\ \eta^{-}\Delta\theta_{ji}^{(q)}(n_{ep}-1) & , \dfrac{\partial\xi_{av}}{\partial\theta_{ji}^{(q)}}(n_{ep}-1)\dfrac{\partial\xi_{av}}{\partial\theta_{ji}^{(q)}}(n_{ep}) < 0 \end{cases} \tag{12}$$

where $0 < \eta^{-} < 1 < \eta^{+}$. If the partial derivative changes signs from one epoch to other, the weight-update size is decreased by η^{-}; otherwise it is increased by η^{+}. The LM algorithm (Hagan, Menhaj, 1994) is a batch learning technique that minimizes the average error energy by updating the network weights after every epoch. The weight updating in the NN training using the LM algorithm is:

$$\Delta\boldsymbol{\theta}(n_{ep}) = \left[\mathbf{J}^{T}(\boldsymbol{\theta})\mathbf{J}(\boldsymbol{\theta}) + \mu\mathbf{I}\right]^{-1}\mathbf{J}^{T}(\boldsymbol{\theta})\boldsymbol{\xi}(n_{ep}) \tag{13}$$

where, $\boldsymbol{\theta} = \left[\theta_{11}^{(1)},...,\theta_{ji}^{(q)},...\right]^{T}$ is the network weigh-vector, $\boldsymbol{\xi} = \left[\xi(1),...,\xi(p),...,\xi(P)\right]^{T}$ is the error energy vector, μ is the regularization parameter, $\mathbf{I}$ is the identity matrix; and $\mathbf{J}(\boldsymbol{\theta})$ is the Jacobian matrix, defined as:

$$\mathbf{J}(\boldsymbol{\theta}) = \begin{bmatrix} \partial\xi(1)/\partial\theta_{11}^{(1)} & \dots & \partial\xi(1)/\partial\theta_{ji}^{(q)} & \dots \\ \vdots & & \vdots & \\ \partial\xi(P)/\partial\theta_{11}^{(1)} & \dots & \partial\xi(P)/\partial\theta_{ji}^{(q)} & \dots \end{bmatrix} \tag{14}$$

Once all the examples of the training sample are fed to the network, the error energy vector and the Jacobian matrix are computed for weight updating. Then the error energy vector is again computed with recent updated weights. If the resultant new errors are alleviated, then the regularization parameter μ is divided by the factor δ; otherwise vice-versa for next epoch (Hagan & Menhaj, 1994; Seyman & Taspinar, 2013).

4 SIMULATION RESULTS

FOR the Monte-Carlo simulation under various fading scenarios, the fade-rates and different values of the signal-to-noise-ratio (SNR), a 4×1 SFBC-OFDM system with 4-QAM scheme $N = 64$ and $G = 16$ (CP) is considered that corresponds to the work of Ye, Li, & Juang, 2018. The QAM symbols are then encoded for 4-transmit antennas using the QO-STBC scheme (as in Equation 1). The ANN is trained using a $P = 50$ SFBC-OFDM symbol block as a training sample (epoch). Each example in a training sample is first fed to the NN for the output and error calculations, which are utilized for weight updating after each epoch (after averaging errors from all examples in an epoch). The received signal and originally transmitted signal for the first 50 SFBC-OFDM blocks are treated as training data. The input to ANN model is the received signal, and the model is trained to reduce (by iterative process) the difference between the network output and originally transmitted signal (Ye, Li, & Juang, 2018).

4.1 BER Performance of ANN Algorithms at Different Fade-rate and SNR Values

For the GDM algorithm, the learning-rate and momentum constant are considered to be $\eta = 0.1$ and

$\alpha = 0.01$, respectively, for both the FFNN and RNN. For the RProp algorithm, the initial learning rate is kept at $\eta = 0.95$ for the FFNN, $\eta = 0.1$ for the RNN, with $\eta^{+} = 1.2$ and $\eta^{-} = 0.5$. The initial value of the regularization parameter in the LM algorithm is set at $\mu = 0.95$ for the FFNN, $\mu = 0.1$ for RNN, and δ =10. The fade-rate =0.0001 at SNR, =+25dB for FFNN, and the BER value in case the LM algorithm is 0.0017 (as illustrated in Figure 4), which provides approximately +1dB performance advantage over the MF approach under similar conditions. However, the BER =0.0021 for the RProp and the BER =0.0035 for the GDM algorithm, which are observed under the same scenario. For the RNN, the BER values are 0.0010, 0.0013, and 0.0021 and for the LM, RProp and GDM algorithms respectively, which is in the close vicinity to BER =0.001 and for the LS algorithm (as shown in Figure 5).

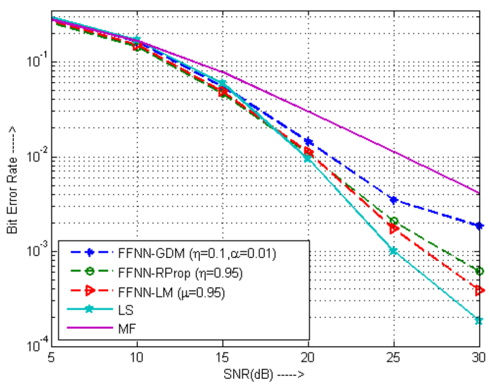

Figure 4. BER vs. SNR for the FFNN at the Fade-rate of = 0.0001.

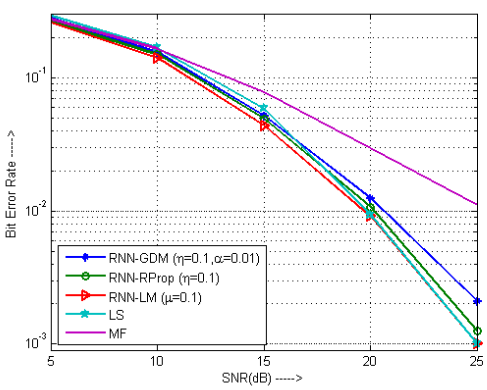

Figure 5. The BER vs. the SNR for the RNN at the Fade-rate of = 0.0001.

For the fade-rate to =0.001 and the BER =0.01 and in case of the LM algorithm, its performance advantage in terms of the SNR is approximately 3dB for the FFNN and 4.5dB for the RNN in comparison to the MF approach (Rouquette, Mérigeault, & Gosse, 2002) (as depicted in Figures 6 and 7). The RNN provides better symbol recovery with a SNR advantage of approximately +1dB for LM, 0.5dB for the Rprop and 1.75dB for the GDM algorithms, at the BER of =0.01, in comparison to the FFNN. The LS algorithm performs approximately +1dB better than the LM algorithm in the RNN at a fade-rate of =0.001 and the BER of =0.01. It is evident from Figure 8 that as the fade-rate elevates, the BER performance gets deteriorated for all the algorithms, but the performance of the RNN supersedes the FFNN. However, the LM algorithm apparently outperforms the RProp as well as the GDM algorithms by providing a lower BER under similar conditions, such that the BER(LM) < BER(RProp) < BER(GDM). Table 1 illustrates the BER performance of various ANN algorithms at different fade-rates for distinct values of the SNR.

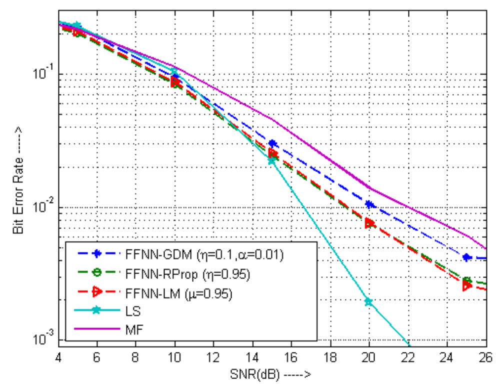

Figure 6. The BER vs. SNR for the FFNN at the fade-rate of = 0.001.

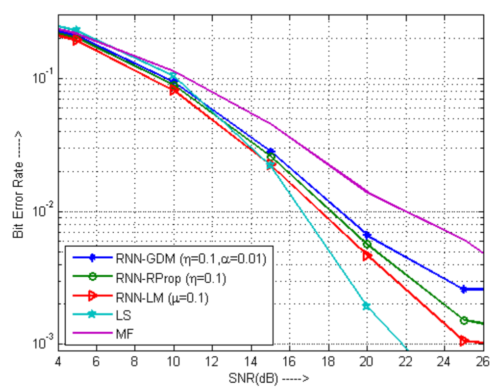

Figure 7. The BER vs. the SNR for the RNN at the fade-rate of = 0.001.

Table 1. **The BER Values of Different ANN Algorithms at Distinct Values of the Fade-rate for the Fixed SNR.**

Fade-Rate	FFNN-LM		FFNN-RP		FFNN-GDM		RNN-LM		RNN-RP		RNN-GDM	
	BER at fixed SNR		BER at fixed SNR		BER at fixed SNR		BER at fixed SNR		BER at fixed SNR		BER at fixed SNR	
	+27.5 dB	+22.5 dB	+27.5 dB	+22.5 dB	+27.5 dB	+22.5 dB	+27.5 dB	+22.5 dB	+27.5 dB	+22.5 dB	+27.5 dB	+22.5 dB
0.00001	0.00089	0.005	0.00124	0.00576	0.00188	0.00672	0.000359	0.00375	0.000448	0.00449	0.00121	0.00589
0.00005	0.00124	0.0048	0.001548	0.00535	0.002569	0.00583	0.000494	0.00296	0.000705	0.00367	0.00196	0.00507
0.0001	0.00076	0.004	0.000964	0.00455	0.001757	0.0066	0.000528	0.0027	0.000765	0.0036	0.001655	0.005
0.0005	0.00089	0.0013	0.001134	0.001619	0.001886	0.0022	0.000317	0.001264	0.000584	0.00149	0.001401	0.00221
0.001	0.002396	0.003	0.002599	0.003758	0.004237	0.00446	0.000973	0.00263	0.001314	0.0032	0.002184	0.00491
0.005	0.078151	0.0827	0.07728	0.08593	0.090127	0.09634	0.08173	0.0797	0.090985	0.0897	0.098272	0.09602
0.01	0.21099	0.2198	0.20367	0.2195	0.23222	0.2402	0.20323	0.2132	0.21462	0.2237	0.2265	0.2391

4.2 *BER Performance for Different Quasi-orthogonal Codes*

The performance of the ANN based equalisation in the SFBC-OFDM system is also analysed using various quasi-orthogonal block codes, in which, the different distribution of conjugates in the transmission matrix results in distinct positions of the correlated values (Hou, Lee, & Park, 2003). In this paper, different QO-STBC schemes are incorporated in the underlying SFBC-OFDM system under similar conditions. These schemes are the Jafarkhani code (Jafarkhani, 2001), the Tirkkonen–Boariu–Hottinen (TBH) code (Tirkkonen, Boariu, & Hottinen, 2000), the Jafarkhani with TBH correlated positions code, and the TBH with Jafarkhani correlated positions code (Hou, Lee, & Park, 2003).

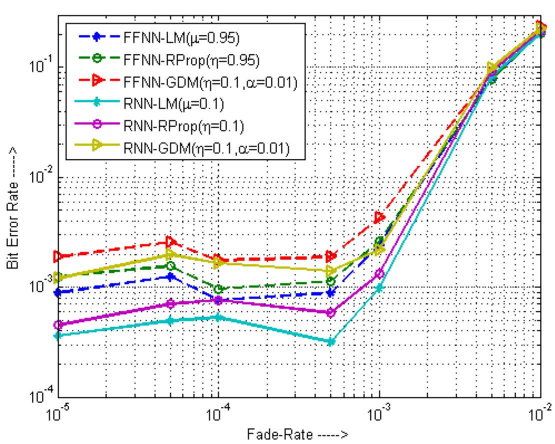

Figure 8. **The BER vs. the Fade-rate at the Fixed SNR of = +27.5dB.**

It is quite evident from the results demonstrated in Figure 9 that the BER performance of the underlying system is approximately similar for the aforementioned four QO-STBC codes, while using the recurrent neural network architecture with the LM training algorithm for equalization. The results are in close agreement with the observation reported by Su & Xia (2002). Under the typical channel conditions, the performance of the TBH based QO-STBC codes (Tirkkonen, Boariu, & Hottinen, 2000) is observed to be deteriorated (Hou, Lee, & Park, 2003); but in combination with the OFDM system, their performance improves significantly, as the DFT operation at the receiver in the OFDM system randomizes the interference/noise terms (Grover, Kapoor & Kohli, 2012). However, the QO-STBC based codes pioneered by Jafarkhani (Jafarkhani, 2001) always perform well, with or without the OFDM based system configuration, even under the adverse fading environment.

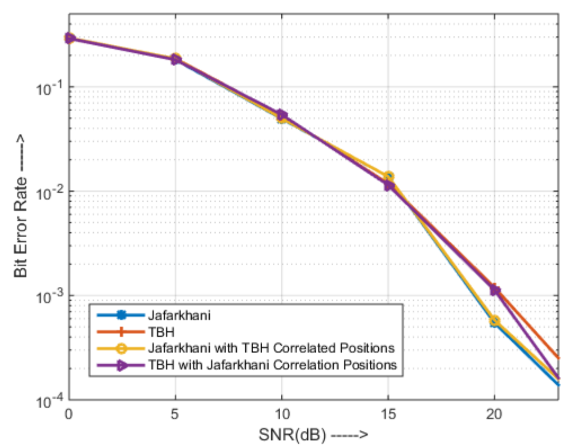

Figure 9. **The BER for QO-codes at the Fade-rate of = 0.0001.**

5 CONCLUDING REMARKS

AN ANN based intelligent receiver for a 4×1 SFBC-OFDM system is explored, which detects the transmitted symbols directly from the received signal under the slowly time-varying multipath environment. It precludes the usage of the channel estimation. The simulation results connote that the RNN configuration with the LM and RProp algorithms has an edge over the FFNN under similar conditions for different fade-rate and SNR values, in terms of the lower BER. The performance of the RNN with the GDM algorithm is found to be better than the FFNN with GDM, but its performance is quite inferior to the LM and RProp algorithms. The results for the 4×1 SFBC-OFDM systems manifest that the recurrent architecture with the LM algorithm outperforms all other discussed ANN algorithms by exhibiting comparatively a lower BER. However, some distinct QO-STBC codes may be utilized in underlying the SFBC-OFDM system, but the QO-STBC codes proposed by Jafarkhani undoubtedly appears to be the best choice. The future scope includes the applications of the presented channel equalization based intelligent SFBC-OFDM technique in the radio-over-fiber transmission systems using millimeter waves (Habib et. al., 2017; Liu et. al., 2017; Zhu et. al., 2013) and under various fading scenarios (Kapoor & Kohli, 2015; Kapoor & Kohli, 2018; Kohli & Lamba, 2018).

6 DISCLOSURE STATEMENT

NO potential conflict of interest is reported by the authors.

7 REFERENCES

Grover, A., Kapoor, D. S., & Kohli, A. K. (2012). Characterisation of impulse noise effects on space-time block-coded orthogonal frequency division multiplexing (OFDM) signal reception. *International Journal of Physical Sciences*, *7*(25), 4003-4011.

Habib, U., Aighobahi, A. E., Nair, M., Zhu, H., Quinlan, T., Walker, S. D., & Gomes, N. J. (2017). Performance improvement for OFDM-RoF transported 60 GHz system using spatial diversity and multiplexing. In *Communications Workshops (ICC Workshops), 2017 IEEE International Conference on* (pp. 211-216). IEEE.

Hagan, M. T., & Menhaj, M. B. (1994). Training feedforward networks with the Marquardt algorithm. *IEEE transactions on Neural Networks*, *5*(6), 989-993.

Haykin, S. (2009). *Neural networks and learning machines* (Vol. 3). Upper Saddle River, NJ, USA: Pearson.

Hou, J., Lee, M. H., & Park, J. Y. (2003). Matrices analysis of quasi-orthogonal space-time block codes. *IEEE Communications Letters*, *7*(8), 385-387.

Jafarkhani, H. (2001). A quasi-orthogonal space-time block code. *IEEE Transactions on Communications*, *49*(1), 1-4.

Kapoor, D. S., & Kohli, A. K. (2015). Simulation of basis expansion model for channel fading using AR1 process. *Wireless Personal Communications*, *85*(3), 791-798.

Kapoor, D. S., & Kohli, A. K. (2018). Channel estimation and long-range prediction of fast fading channels for adaptive OFDM system. *International Journal of Electronics*, *105*(9), 1451-1466.

Kohli, A. K., & Kapoor, D. S. (2016). Adaptive filtering techniques using cyclic prefix in OFDM systems for multipath fading channel prediction. *Circuits, Systems, and Signal Processing*, *35*(10), 3595-3618.

Kohli, A. K., & Lamba, G. S. (2018). Impact of phase noise on single-tap equalization for fast–OFDM signals under generic linear fading channels. *Optik*, *169*, 382-391.

Kohli, A. K., & Mehra, D. K. (2006). Tracking of time-varying channels using two-step LMS-type adaptive algorithm. *IEEE Transactions on Signal Processing*, *54*(7), 2606-2615.

Lee, K. F., & Williams, D. B. (2000). A space-frequency transmitter diversity technique for OFDM systems. In *Global Telecommunications Conference, 2000. GLOBECOM'00. IEEE* (Vol. 3, pp. 1473-1477). IEEE.

Liu, S., Xu, M., Wang, J., Lu, F., Zhang, W., Tian, H., & Chang, G. K. (2017). A multilevel artificial neural network nonlinear equalizer for millimeter-wave mobile front haul systems. *Journal of Lightwave Technology*, *35*(20), 4406-4417.

Nawaz, S. J., Mohsin, S., & Ikaram, A. A. (2009). Neural network based MIMO-OFDM channel equalizer using comb-type pilot arrangement. In *Future Computer and Communication, 2009. ICFCC 2009. International Conference on* (pp. 36-41). IEEE.

Riedmiller, M., & Braun, H. (1993). A direct adaptive method for faster backpropagation learning: The RPROP algorithm. In *Neural Networks, 1993. IEEE International Conference on* (pp. 586-591). IEEE.

Rouquette, S., Mérigeault, S., & Gosse, K. (2002). Orthogonal full diversity space-time block coding based on transmit channel state information for 4 Tx antennas. In *Communications, 2002. ICC 2002. IEEE International Conference on* (Vol. 1, pp. 558-562). IEEE.

Seyman, M. N., & Taspinar, N. (2012). Channel estimation based on neural network with feedback for MIMO OFDM mobile communication systems. *Intelligent Automation & Soft Computing*, *18*(3), 307-316.

Seyman, M. N., & TasPınar, N. (2013). Channel estimation based on neural network in space time block coded MIMO–OFDM system. *Digital Signal Processing*, *23*(1), 275-280.

Singh, S., & Kohli, A. K. (2014). Wireless fading paradigm for antenna array receiver for a disk-type cluster of scatterers. *Circuits, Systems, and Signal Processing*, *33*(4), 1231-1244.

Su, W., & Xia, X. G. (2002, November). Quasi-orthogonal space-time block codes with full diversity. In *Global Telecommunications Conference, 2002. GLOBECOM'02. IEEE* (Vol. 2, pp. 1098-1102). IEEE.

Tirkkonen, O., Boariu, A., & Hottinen, A. (2000). Minimal non-orthogonality rate 1 space-time block code for 3+ Tx antennas. In *2000 IEEE Sixth International Symposium on Spread Spectrum Techniques and Applications. ISSTA 2000. Proceedings (Cat. No. 00TH8536)* (Vol. 2, pp. 429-432). IEEE.

Ye, H., Li, G. Y., & Juang, B. H. (2018). Power of deep learning for channel estimation and signal detection in OFDM systems. *IEEE Wireless Communications Letters*, *7*(1), 114-117.

Zhu, M., Zhang, L., Wang, J., Cheng, L., Liu, C., & Chang, G. K. (2013). Radio-over-fiber access architecture for integrated broadband wireless services. *Journal of Lightwave Technology*, *31*(23), 3614-3620.

8 NOTES ON CONTRIBUTORS

Divneet Singh Kapoor received the B.E. degree and M.E. degree in Electronics and Communication Engineering (ECE) from Thapar Institute of Engineering and Technology (TIET, Deemed University), Patiala in 2009 and 2011 respectively. He is serving as an Assistant Professor in ECE department at Chandigarh University, Gharuan (Punjab). He received teaching assistantship/scholarship in M.E. & Ph.D. for good academic performance. He is author as well as reviewer of various research papers published in the distinguished international journals of Springer, Taylor & Francis and IEEE magazine etc., and his six patents are under review.

Amit Kumar Kohli received the B.Tech. (Honor) degree from Guru Nanak Dev Engineering College, Ludhiana (previously affiliated to Punjab University Chandigarh), the M.E. (Highest Honor) degree from Thapar Institute of Engineering and Technology (TIET, Deemed University), Patiala, Punjab and the Ph.D. degree from Indian Institute of Technology, Roorkee, India, in 2000, 2002 and 2006 respectively, all in Electronics and Communication Engineering (ECE). He is presently Associate Professor and Student-Mentorship Coordinator in ECE department of TIET Patiala, India. He served as Member of Senate, Member of Staff Affairs Committee as well as Member of Board of Governors, and also served as Post-graduation Coordinator ECE department, TIET Patiala, India.

His research interests include signal processing & its applications, wireless & high data-rate advanced communication systems, neural networks & bio-medical engineering and adaptive system design & machine learning. He has already supervised four Ph.D. and thirty nine M.E. dissertations, and has also authored more than sixty seven research publications in the distinguished international journals/transactions of IEEE, Springer, Taylor & Francis and Elsevier etc. He received National Scholarship, State Scholarship, GATE / MHRD Fellowship, Institution Medal, and Gold Medal consecutively for academic performance.